Available online at www.sciencedirect.com
ScienceDirect
Applied Surface Science 252 (2006) 7608–7613
applied surface science
www.elsevier.com/locate/apsusc

Computing surface dipoles and potentials of self-assembled monolayers from first principles

Amir Natan [a], Leeor Kronik [a,*], Yoram Shapira [b]

[a] Department of Materials and Interfaces, Weizmann Institute of Science, Rehovoth 76100, Israel
[b] Department of Physical Electronics, Tel-Aviv University, Ramat Aviv 69978, Israel

Available online 14 June 2006

Abstract

We discuss methodological aspects of first principles calculations of surface dipoles and potentials in general, and surface-adsorbed self-assembled monolayers in particular, using density functional theory with a slab/super-cell approach. We show that calculations involving asymmetric slabs may yield highly erroneous results for the surface dipole and demonstrated the efficacy of a simple dipole correction scheme. We explain the importance of the electrostatic dipole *distribution*, show how to compute it, and establish conditions for the equivalence of calculations for the dipole distribution and the electrostatic potential distribution.
© 2006 Elsevier B.V. All rights reserved.

Keywords: Density functional theory; Dipole layer; Work function; Self-assembled monolayers

1. Introduction

The performance of most semiconductor devices is critically dependent on the electronic properties of semiconductor surfaces and/or interfaces [1]. Use of organic or organometallic molecules that are surface-adsorbed as self-assembled monolayers (SAMs) is a potentially powerful and flexible approach to fine-tuning the desired electronic properties of surface and interfaces. Indeed, control over surface [2–4] and interface [5–8] electronic structure via SAMs has been successfully demonstrated.

A key phenomenon associated with semiconductor/SAM interfaces is the modification of the surface dipole. SAM-related surface dipoles – and the overall system response to them – have recently been invoked as the controlling factor in arenas as diverse as charge transport [5–8], chemically sensitive field effect transistors [9], novel interface magnetic phenomena [10,11], and even molecular nano-patterning [12].

In light of the rising importance of molecular SAM in semiconductor interfaces, it is reasonable to attempt an understanding and rational design of SAM-containing interface electronic properties in general, and dipoles in particular, using first principles calculations [13–15]. This is especially so given that first principles calculations based on density functional theory (DFT) have become a powerful tool for explaining and predicting the properties of bulk [16], surface [17], and molecular [18] systems.

DFT studies of surfaces often employ a planewave basis, where a ''super-cell'' geometry with three-dimensional periodic boundary conditions is used [17]. Because the real system is periodic in only two dimensions, a slab geometry is used, i.e., a vacuum layer that is sufficiently large to avoid spurious interaction between the ''front'' and ''rear'' surfaces of the slab is inserted in the periodic cell. An example of a slab/super-cell geometry for a nitrobenzene SAM adsorbed on the Si(1 1 1) surface is shown in Fig. 1.

As discussed in detail below, a successful computation of surface dipoles (and corresponding surface potentials) within the planewave-DFT framework presents special challenges that are often not discussed in the analysis of specific systems. The purpose of this article is to provide a systematic discussion of the computations of surface dipoles and potentials in general and surface-adsorbed SAMs in particular. The paper is arranged as follows: first, we discuss the computation of total dipole moments; next, we discuss the computation of partial dipole moments and finally, we discuss the computation of the surface potential and its relation to the surface dipole. Our considerations are illustrated throughout the paper by numerical

* Corresponding author. Tel.: +972 8 934 4993; fax: +972 8 934 4138.
E-mail address: leeor.kronik@weizmann.ac.il (L. Kronik).

0169-4332/$ – see front matter © 2006 Elsevier B.V. All rights reserved.
doi:10.1016/j.apsusc.2006.03.052

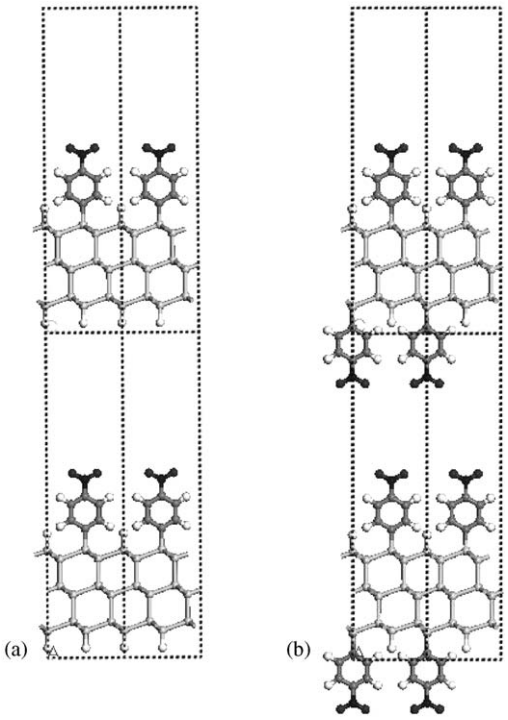

Fig. 1. An example of a super-cell/slab geometry for surface studies—a nitrobenzene SAM adsorbed on the Si(1 1 1) surface. (a) A one-sided slab configuration: six layers of silicon with a nitrobenzene-adsorbed top surface and a hydrogen-passivated bottom surface. (b) A symmetric slab configuration: six layers of silicon with nitrobenzene adsorbed on both surfaces.

examples taken from calculations of the nitrobenzene SAM/Si(1 1 1) system of Fig. 1.

2. Computing total dipoles

Naively, the easiest way to assess surface dipole modifications brought about by the adsorption of a molecular SAM is to use the asymmetric slab configuration shown in Fig. 1a. In this configuration, one surface is a reference, well-passivated surface (e.g., hydrogen-passivated for the case of a silicon surface) and the other surface is the SAM-adsorbed one. The calculation of P_z, the total dipole for such a slab, then appears to be straightforward, given simply by the overall dipole of the super-cell in direction perpendicular to the surface (which we define to be the z axis):

$$P_z = \int_0^{z_{\text{cell}}} z' \bar{\rho}(z')\, \mathrm{d}z', \tag{1}$$

where

$$\bar{\rho}(z) = \iint_A \rho(x, y, z)\, \mathrm{d}x\, \mathrm{d}y \tag{2}$$

is the xy-plane integrated charge density, $\rho(x, y, z)$ is the combined ionic and electronic charge density in the super-cell, and the super-cell extends from 0 to z_{cell} in the z direction.

Eq. (1), however, suffers from a major flaw [19–22]: elementary electrostatics shows that a finite dipole extending in two dimension results in a finite potential step across the dipole. This means that physically there must be a potential difference across the super-cell. However, such a difference is prohibited mathematically because of the periodic boundary condition in the z direction. As a result, a spurious electric field is set up so that the boundary condition is obeyed. This field is directly dependent on the total dipole and is easily shown to be given by [21]:

$$E_z = 4\pi \frac{P_z}{A z_{\text{cell}}} = 4\pi \frac{P_z}{V_{\text{cell}}}, \tag{3}$$

where A is the super-cell area in the xy plane and V_{cell} is the super-cell volume. It has been long recognized that this spurious field results in a very slow convergence of the total energy with super-cell size [20]. However, we are not aware of a discussion of the spurious field effect on surface *dipoles*. Unfortunately, the error can be particularly severe for SAMs because the adsorbed molecules often have a significant polarizability, i.e., an electric-field induced polarization. This means that, to first order, the dipole calculated from Eq. (1), P_z, will be related to the true dipole, P_z^0, via:

$$P_z = P_z^0 + \alpha E_z, \tag{4}$$

where α is an effective polarizability. Inserting E_z from Eq. (3) and solving for P_z we obtain:

$$P_z = \frac{P_z^0}{1 - 4\pi\alpha / V_{\text{cell}}}. \tag{5}$$

Thus, the higher the SAM polarizability, the worse its dipole will be overestimated. Furthermore, the electronic structure of highly polarizable molecules may change significantly in reaction to the spurious field, resulting in a quantitatively, and possibly even qualitatively, incorrect computed electronic structure of the SAM/substrate interface.

There are two known remedies to the spurious field problem: One is to correct for the total energy a posteriori [20]. This is not helpful in the present case, because we are interested in the dipole itself and not just in its effect on the energy. The other remedy is to place an additional dipolar sheet far enough inside the vacuum region, such that the overall dipole across the super-cell is now zero, and modify the upper limit for the integral in Eq. (1) accordingly [21]. The latter approach involves the introduction of an extra charge-dependent term in the Hamiltonian of the self-consistent problem to be solved. This is no problem in principle, although our experience with employing this correction suggests that it occasionally results in convergence problems [23].

As a concrete example for the magnitude of the errors involved, we calculated [23] the dipole of a periodic two-dimensional array of nitro-benzene molecules, with one molecule per super-cell, for various super-cell dimensions. For simplicity, we used the molecular gas phase structure and did not include an underlying substrate. The results of the calculations, with and without a dipole correction, are given in Table 1. We note that, computational artifacts aside, we do expect the dipole of this array to decrease with decreasing

Table 1
Calculation of the surface dipole for a periodic array of nitrobenzene molecules with one molecule per cell, with and without an explicit dipole correction

Cell size (Å)	Dipole with correction (D)	Dipole without correction (D)	Energy difference (eV)
3.83 × 6.64 × 20	2.58	3.32	0.07
7.44 × 6.64 × 20	3.27	3.87	0.05
10.58 × 10.58 × 15.87	3.98	4.48	0.04

Total energy differences due to the dipole correction are also given.

lateral distance between molecules due to dipole–dipole depolarization effects [15]. This is indeed clearly observed. However, omitting the dipole correction causes a very significant overestimate of the dipole, by 0.5–0.7 D, in agreement with the prediction of the phenomenological Eq. (5). This is despite the fact that the associated total energy change is a much more modest 0.04–0.07 eV, highlighting the need for explicit dipole correction.

3. Computing partial dipoles

A different route to avoiding spurious dipole calculations is to use a symmetric slab, as shown in Fig. 1b, whose total dipole is inherently zero. This appears to be a waste of computational resources. However, this approach is free of the above-mentioned convergence issues of calculations with a complete dipole correction and may therefore be efficient in practice.

Because the total dipole in this approach is zero, the calculation of partial dipole values within the structure is now necessary. In fact, such calculations are often desirable even when employing asymmetric slabs because they yield information about the *evolution* of the surface dipole along the structure and point to regions where its build-up is particularly significant. For example, one can then tell which part of the dipole drops on the SAM and which part drops on the semiconductor substrate.

We found it convenient to evaluate all dipoles against a vacuum reference plane, such that in the vacuum the dipole is zero by construction and all partial dipoles are given with respect to the vacuum. The partial dipole at an arbitrary plane z in the super-cell is then given by [24]:

$$P_z(z) = \int_z^{z_{\text{cell}}} z' \bar{\rho}(z')\, \mathrm{d}z'. \tag{6}$$

It is important to note that while Eq. (6) is *mathematically* well-defined, it is *physically* well-defined *only* in z planes that divide the overall structure into two neutral sub-units (e.g., the middle point of various bonds). For all other planes, the overall charge between z and z_{cell} is not zero. Thus, the result of Eq. (6) would depend on the choice of origin so that, e.g., moving the slab with respect to the super-cell edges would change the dipole. Furthermore, Eq. (6) does not offer a simple way of locating the physically meaningful z planes. However, such a location is easy with a slight modification of Eq. (6):

$$P_z(z) = \int_z^{z_{\text{cell}}} (z' - z) \bar{\rho}(z')\, \mathrm{d}z'. \tag{7}$$

Eqs. (6) and (7) are, in general, not equivalent. However, at the physically meaningful z planes (that divide the structure to two neutral sub-units) Eqs. (6) and (7) will yield identical results because $\int_z^{z_{\text{cell}}} \bar{\rho}(z')\, \mathrm{d}z' = 0$ by definition. Differentiating Eq. (7) with respect to z, we obtain:

$$\frac{\mathrm{d}P_z(z)}{\mathrm{d}z} = -\int_z^{z_{\text{cell}}} \bar{\rho}(z')\, \mathrm{d}z'. \tag{8}$$

Eq. (8) shows that physically meaningful dipole values are obtained from Eq. (7) at and only at z values for which $P_z(z)$ is at an extremum, for only then is the right hand side zero and the structure is divided into neutral sub-units.

Another advantage of Eq. (7) over Eq. (6) is that it is much more stable numerically, because in Eq. (6) small deviation in the charge density can be weighted by a large z value and introduce a large error. This is a serious problem in practice because most planewave codes provide the charge density on a finite grid that does not generally correspond to the physically meaningful z planes.

As an example of the foregoing considerations, we consider the evolution of the dipole for the symmetric nitrobenzene SAM/Si(1 1 1) surface shown in Fig. 1b. Partial dipoles have been evaluated using both Eqs. (6) and (7). The results are given

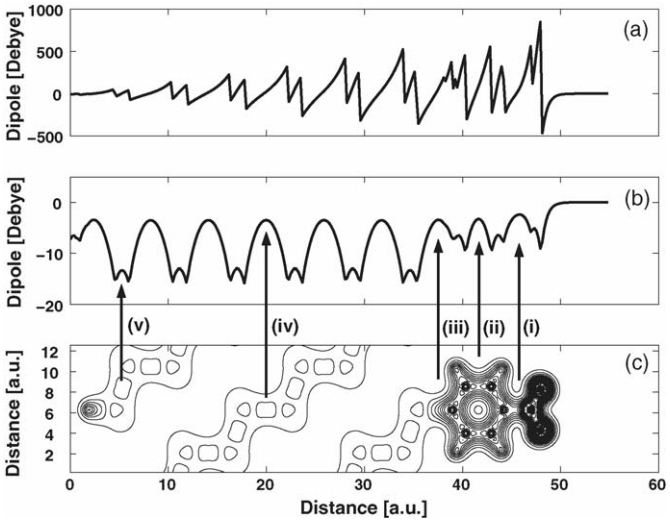

Fig. 2. (a + b) Calculated electrostatic dipole perpendicular to the surface as a function of position inside the structure, using (a) Eq. (6) and (b) Eq. (7). (c) Charge density map in the yz plane for the same configuration. The special planes (i)–(v) contain the middle of the C–N bond, the C–C bond in the center of the benzene ring, the Si–C bond, a Si–Si bond inside the bulk that is perpendicular to the x–y plane, and a Si–Si bond inside the bulk that is nearly parallel to the x–y plane, respectively.

in Fig. 2. Clearly, dipoles obtained with Eq. (6) (Fig. 2a) are too numerically sensitive to yield any useful information. Dipoles obtained with Eq. (7) (Fig. 2b), however, are numerically stable. Fig. 2b additionally shows that much of the formed dipole is formed in the functional (nitro) group itself, but a significant fraction of it is formed in the benzene ring and its full value is obtained only inside the silicon.

Comparison of the dipole evolution with a charge density map in the *yz* plane (given in Fig. 2c) reveals that, in agreement with Eq. (8), many extremal points correspond to *z* planes that obviously do divide the slab into neutral sub-units, such as planes perpendicular to bond centers. The special *z* planes correspond to both ''higher'' local maxima (e.g., point (iv) in Fig. 2) and ''lower'' local maxima (e.g., point (v) in Fig. 2) of the dipole curve. The ''higher'' maxima planes are perpendicular to bonds, whereas the ''lower'' maxima planes are not and hence result in a different partial dipole value. Interestingly, Leung et al. [24] used Eq. (6) for dipole evaluation. They recommended, without proof, that the lower limit for integration ''be chosen to be the mid point between any two layers that are deep in the bulk''. The above discussion provides a rationale for this choice. Importantly, the difference between the ''high'' and ''low'' locally maximal dipole values is very large—about 9.5 D. This means that a consistent reference point (which we chose, for reasons elaborated below, as the ''high'' maxima planes in the bulk) should be used when comparing different SAMs.

As a further demonstration of the additional information inherent in a partial dipole calculation, we computed the partial dipole distribution of a symmetric slab and compared it to the total dipole of an asymmetric slab (calculated with a full dipole correction) where the bottom surface was passivated with hydrogen atoms, for several different SAMs. The comparison yielded values that were shifted consistently by 1.8 D (with a deviation smaller than 0.01 D). This deviation is due to the dipole of the passivated surface. As there are two Si–H bonds per super-cell, we estimate the dipole of an individual surface Si–H bond at the particular geometry [15] shown in Fig. 1a to be 0.9 D.

4. From dipoles to potentials

We now turn to assessing the surface dipole effect on the surface potential. This is important, because surface potential modifications are reflected in the surface work function—an important quantity that is easily accessible experimentally [4].

Because of the lateral periodicity of the charge density, it may Fourier-expanded in the *x* and *y* coordinates, in the form [21]:

$$\rho(x,y,z) = \frac{\bar{\rho}(z)}{A} + \sum_{G_x,G_y}{}' \rho(z,G_x,G_y)\, \mathrm{e}^{\mathrm{i}(G_x x + G_y y)}, \tag{9}$$

where G_x, G_y are the *x* and *y* components of the super-cell's reciprocal lattice vectors. The Fourier expansion of the electrostatic potential is then easily found by solving the Poisson equation for each Fourier component separately, with the result being [21]:

$$V(x,y,z) = V_{\mathrm{av}}(z) + \sum_{G_x,G_y}{}' V(z,G_x,G_y)\, \mathrm{e}^{\mathrm{i}(G_x x + G_y y)}, \tag{10}$$

where:

$$V_{\mathrm{av}}(z) = -\frac{2\pi}{A}\int_0^{z_{\mathrm{cell}}} \bar{\rho}(z')|z-z'|\,\mathrm{d}z', \tag{11}$$

$$V(z,G_x,G_y) = \frac{2\pi}{\sqrt{G_x^2+G_y^2}} \times \int_0^{z_{\mathrm{cell}}} \mathrm{d}z'\,\rho(z',G_x,G_y)\,\mathrm{e}^{-|z-z'|\sqrt{G_x^2+G_y^2}} \tag{12}$$

Physically, $V_{\mathrm{av}}(z)$ Eq. (11) is the potential obtained if one views the slab as a series of infinitesimal planes, each with a *uniform* charge, with the Fourier components of Eq. (12) revealing how significant the deviation from non-uniformity is. If $|z-z'| > \max(1/\sqrt{G_x^2+G_y^2})$, i.e., larger than the leading lateral dimension of the super-cell, which is typically indeed the case a few Å into the vacuum region, then the contribution of Eq. (12) to the potential is negligible. $V_{\mathrm{av}}(z)$ is therefore a good measure of the surface potential of the monolayer.

We now show that $V_{\mathrm{av}}(z)$, calculated using Eq. (11), is intimately related to $P_z(z)$ calculated from Eq. (7) (but not from Eq. (6)). Assume that the total dipole for the whole slab is P_z (which, as discussed above, must be accompanied in the calculation by a corrective dipole of magnitude—P_z). Then, employing considerations similar to those used in deriving Eq. (7), we obtain:

$$\int_0^z \bar{\rho}(z')|z'-z|\,\mathrm{d}z' = \int_z^{z_{\mathrm{cell}}} \bar{\rho}(z')|z'-z|\,\mathrm{d}z' - P_z \tag{13}$$

Using Eq. (13) in Eq. (11) yields:

$$V_{\mathrm{av}}(z) = -\frac{4\pi}{A}\int_z^{z_{\mathrm{cell}}} \bar{\rho}(z')|z-z'|\,\mathrm{d}z' + \frac{2\pi}{A}P_z, \tag{14}$$

Comparing Eq. (14) to Eq. (7) we find that (to within an uninteresting additive factor that depends on the total dipole and the definition of the zero of potential):

$$V_{\mathrm{av}}(z) = -\frac{4\pi}{A}P_z(z) \tag{15}$$

To demonstrate Eq. (15), Fig. 3 shows the average electrostatic potential for the asymmetric, dipole corrected nitrobenzene SAM/Si(1 1 1) system. The average potential is calculated both by averaging the electrostatic potential directly and by computing it from the dipole using Eqs. (7) and (15). Clearly, the two curves are nearly identical around the ''high'' maxima and in the vacuum region, except at and beyond the dipole correction sheet (see special plane (vi) in the figure), as this sheet is not represented in the charge density of the actual system. However, there are additional differences. The potential calculated by direct averaging features distinct minima, whereas the one computed from the dipole features cusps and ''low'' maxima

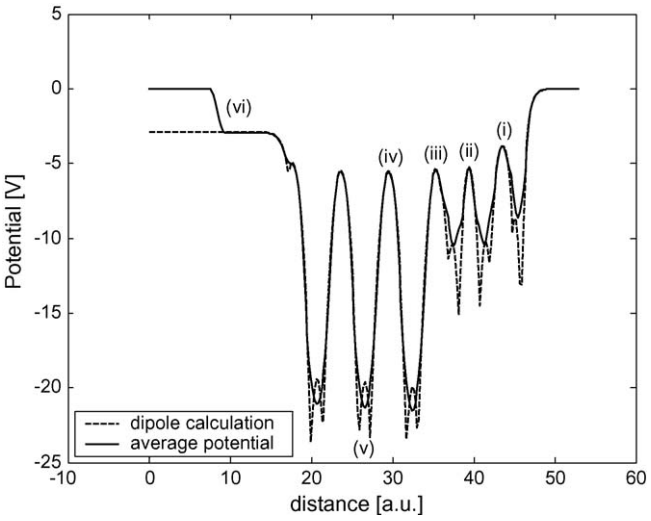

Fig. 3. Comparison of averaged electrostatic potential computed by explicit averaging of the potential (solid line) and from the average dipole (dashed line). The special planes (i)–(v) contain the middle of the C–N bond, the C–C bond in the center of the benzene ring, the Si–C bond, a Si–Si bond inside the bulk that is perpendicular to the *x*–*y* plane, and a Si–Si bond inside the bulk that is nearly parallel to the *x*–*y* plane, respectively. The special plane (vi) indicates the position of the dipole correction sheet.

instead. These differences arise despite the formal identity of the two calculations demonstrated in Eq. (15), for the following physical reason: When using Eq. (7), the ionic charge density is added as a set of point charges to the electronic charge density. However, the DFT calculations performed here additionally replace the nuclear charge and core electrons by an approximate treatment [23] that causes a smoothing of the electrostatic potential. Because this causes both the electrostatic potential and the charge density to differ from their true values in the vicinity of the nuclei, neither calculation is rigorously valid in that region.

The preceding argument establishes rigorously that the computation of the averaged electrostatic potential, together with Eq. (15), may be used as a possibly easier alternative to a direct calculation of the dipole. It also establishes that using either dipoles or average potentials, the extrema *between* the nuclei in the bulk should be used as reference. We emphasize that as long as we are interested in *relative* changes in the work function (e.g., upon adsorption of a monolayers), comparing surface dipoles and potentials using this reference point is a valid approach. If one is interested in an *absolute* value, the position of the bulk Fermi level needs to be determined additionally, as has been discussed in detail elsewhere [25].

5. Conclusions

In conclusion, we provided a systematic discussion of first principles computation of surface dipoles and potentials in general and surface-adsorbed SAMs in particular, using DFT with a slab/super-cell approach. We explained why calculation of an asymmetric slab may yield highly erroneous results for the surface dipole and demonstrated the efficacy of a simple correction scheme. We explained the importance of the electrostatic dipole distribution, showed how to compute it, and established conditions for the equivalence of calculations for the dipole distribution and the electrostatic potential distribution.

Acknowledgements

We thank Lior Segev for many helpful discussions. L.K. acknowledges financial support from the Israel Science Foundation (“Bikura”), the Minerva Foundation, the Gerhard Schmidt Minerva Center for Supra-Molecular Architecture, the “Phoremost” European Network of Excellence, and the Delta Career development chair.

References

[1] See, e.g. S.M. Sze, Physics of Semiconductor Devices, second ed., Wiley, New York, 1981.
[2] M. Bruening, R. Cohen, J.F. Guillemoles, T. Moav, J. Libman, A. Shanzer, D. Cahen, J. Am. Chem. Soc. 119 (1997) 5720;
M. Bruening, E. Moons, D. Yaron-Marcovich, D. Cahen, J. Libman, A. Shanzer, J. Am. Chem. Soc. 116 (1994) 2972.
[3] R. Cohen, L. Kronik, A. Shanzer, D. Cahen, A. Liu, Y. Rosenwaks, J.K. Lorenz, A.B. Ellis, J. Am. Chem. Soc. 121 (1999) 10545;
R. Cohen, L. Kronik, A. Vilan, A. Shanzer, Y. Rosenwaks, D. Cahen, Adv. Mater. 12 (2000) 33.
[4] L. Kronik, Y. Shapira, Surf. Sci. Rep. 37 (1999) 1.
[5] I.H. Campbell, S. Rubin, T.A. Zawodzinski, J.D. Kress, R.L. Martin, D.L. Smith, N.N. Barashkov, J.P. Ferraris, Phys. Rev. B 54 (1996) R14321.
[6] A. Vilan, A. Shanzer, D. Cahen, Nature 404 (2000) 166;
H. Haick, J. Ghabboun, O. Niitsoo, H. Cohen, D. Cahen, A. Vilan, J.Y. Hwang, A. Wan, F. Amy, A. Kahn, J. Phys. Chem. B 109 (2005) 9622.
[7] L. Zuppiroli, L. Si-Ahmed, K. Kamaras, F. Nüesch, M.N. Bussac, D. Ades, A. Siove, E. Moons, M. Grätzel, Eur. Phys. J. B 11 (1999) 505;
J. Krüger, U. Bach, M. Grätzel, Adv. Mater. 12 (2000) 447.
[8] C. Ganzorig, K.-J. Kwak, K. Yagi, M. Fujihira, Appl. Phys. Lett. 79 (2001) 272.
[9] D.G. Wu, G. Ashkenasy, D. Shvarts, R.V. Ussyshkin, R. Naaman, A. Shanzer, D. Cahen, Angew. Chem. Int. Ed. 39 (2000) 4496;
D.G. Wu, D. Cahen, P. Graf, R. Naaman, A. Nitzan, D. Shvarts, Chem. Eur. J. 7 (2001) 1743.
[10] Z. Vager, R. Naaman, Phys. Rev. Lett. 92 (2004) 087205;
I. Carmeli, G. Leitus, R. Naaman, S. Reich, Z. Vager, J. Chem. Phys. 118 (2003) 10372;
T.C. Kreutz, E.G. Gwinn, R. Artzi, R. Naaman, H. Pizem, C.N. Sukenik, Appl. Phys. Lett. 83 (2003) 4211.
[11] P. Crespo, et al. Phys. Rev. Lett. 93 (2004) 087204.
[12] W. Lu, D. Salac, Phys. Rev. Lett. 94 (2005) 146103.
[13] V. De Renzi, R. Rousseau, D. Marchetto, R. Biagi, S. Scanodolo, U. del Pennino, Phys. Rev. Lett. 95 (2005) 046804.
[14] M.F. Iozzi, M. Cossi, J. Phys. Chem. B 109 (2005) 15383.
[15] A. Natan, Y. Zidon, Y. Shapira, L. Kronik, Phys. Rev. B 73 (2006) 193310.
[16] M.L. Cohen, J.R. Chelikowsky, Electronic Structure and Optical Properties of Semiconductors, Springer, Berlin, 1988.
[17] G.P. Srivastava, Theoretical Modelling of Semiconductor Surfaces: Microscopic Studies of Electrons and Phonons, World Scientific, Singapore, 1999;
G.P. Srivastava, Rep. Prog. Phys. 60 (1997) 561.
[18] W. Koch, M.C. Holthausen, A Chemist’s Guide to Density Functional Theory, second ed., Wiley-VCH, Weinheim, 2001.
[19] J. Neugebauer, M. Scheffler, Phys. Rev. B 46 (1992) 16067.

[20] G. Makov, M.C. Payne, Phys. Rev. B 51 (1995) 4014.
[21] L. Bengtsonn, Phys. Rev. B 59 (1999) 12301.
[22] P.A. Schultz, Phys. Rev. B 60 (1999) 1551.
[23] All computational results presented in this paper were obtained using version 4.6 of the Vienna ab initio simulation package (VASP) (G. Kresse, J. Furthmüller, Phys. Rev. B 54 (1996) 11169) while treating the core electrons using the projector augmented wave method (G. Kresse, D. Joubert, Phys. Rev. B 59 (1999) 1758). In particular, our experience with dipole correction schemes is based on the VASP implementation of these schemes.
[24] T.C. Leung, C.L. Kao, W.S. Su, Y.J. Feng, C.T. Chan, Phys. Rev. B 68 (2003) 195408.
[25] C.J. Fall, N. Binggeli, A. Baldereschi, J. Phys. Condens. Matter 11 (1999) 2689.